36 韓國海洋工學會誌 第9卷 第1號 pp. 36~46. 1995. 6.

◉ 論 文

# Numerical Study On Ice/Structure Interaction Behaviour in Dynamic Ice Field

조 철 희*

(94년 12월 5일 접수)

## 극지구조물-빙하 상호 작용에 의한 동적해석

Chul H. Jo*

**Key Words** : ICE FORCE(빙력), SPM, Ice breaking Tanker(쇄빙선) Ice Failure(쇄파괴), Failure Mode(파괴형태)


## Abstract

빙판파괴 형태는 여러 모드(mode)의 합성이며 실제로 한 가지 양식으로 파괴되는 경우는 거의 일어나지 않는다. 이제까지 빙하중 해석 이론이나 방법은 한 가지 양식에 기준하는 것이었다. 이 논문에서는 합성모드로 빙판이 파괴될 때 해양구조물에 작용하는 빙하중 추정방법을 소개하며 모형 실험결과치와 그 결과를 비교하였다.

두 가지 합성모드에 대한 빙하중 추정방법인 비례파괴해석법 (Proportional Failure Method)과 국부경계해석법(Local Ice Boundary Method)을 본논문에 소개하였으며, 이 두 가지 방법과 함께 널리 알려진 Crushing 해석방법을 적용하여 정적 및 동적 구조물에 작용하는 빙하중을 산출/비교하였다. 동적구조물은 쇄빙선을 이용하였고, 쇄빙선이 SPM 터미널에 monopod로 연결되어있는 형태를 선택하였다. 모형 실험은 Finland의 Wartsila실험실에서 실시 하였고, 이 실험을 통하여 쇄빙선에 작용하는 빙력 및 시간별 쇄빙선의 동적 움직임을 측정하였다. 이 논문에서는 위에서 소개된 세가지 방법으로 계산된 빙하중과 실험측정결과를 비교하였고, 이론적으로 추정한 쇄빙선의 운동을 실험결과치와 비교하였다.

Crushing 방법으로 산출한 빙하중은 실제치보다 상당히 높았고, 비례파괴해석법은 Crushing 방법보다 정확한 결과를 보여주었으며, 국부경계해석법은 상당히 모형실험측정치와 가까웠다. 물론 쇄빙선의 움직임도 빙하중에 따라 변화가 심했고, 국부경계해석법을 적용했을 때 실제 쇄빙선의 동적움직임을 가장 가깝게 추정할 수 있었다.


* 현대중공업 해양사업본부

## 1. INTROCUCTION

The increase in oil and gas exploration in Arctic offshore and an increasing level of navigational activities in recent years have generated concerns about how to cope with a wide variety of ice features which may impose a hazard to shipping and to structures in the region. Over the years, studies have been conducted regarding the behaviour of icebreakers and structures operating in ice environment.

Ice forces on structures will vary considerably depending upon ice field conditions, ice speed and various localized interaction modes with ice in contact. Most theories for calculation of ice loads are only for one particular failure mode although usually combinations of failure modes occur in nature. Limitations and application ranges for developed formulas are not very well defined. Also, the classification of ice failure mode is very important in choosing the correct formula. The assumptions and limitations of a formula should be studied and considered carefully before using so that ice loads can be predicted accurately.

Many oil fields are in remote location where harbours do not exist and some type of artificial berths is required for the loading and unloading operations. Various types of terminals have been considered. However, flexibility, reliability and economy make the SPM system the most utilized. The SPM system can be used in severe environmental zones such as rough seas, moving ice, soft seabeds and earthquakes.

Conditions for loading and unloading of tankers are affected by ice contact force and its impact. Tanker movement caused by ice motion should be predicted using ice pressures and ice forces on the tanker. This movement by the tanker affects operation of terminal system. To study the ice forces on the tanker SPM system, the movements of the tanker by ice forces must be known. In the following research the tanker is simplified as a barge. Using a computer simulation of the tanker movement, numerical outputs are obtained and compared with the experimental results.

To predict the ice loads to the tanker moored to an SPM system, three methods(Crushing, Local Ice Boundary and Proportional Failure approaches) are utilized.

## 2. METHODS INTRODUCTION

### 1) Crushing Equation

Korzhavin(1962) proposed the effective ice pressure and force for crushing failure as

$$p = Ikm\left(\frac{V}{V_0}\right)^{-0.333}\sigma_c$$

$$f = pA$$

where I is the indentation coefficient which is 2.5 as ice width is greater than 15D, k contact factor ranging from 0.4 to 0.7, m shape factor which is 1 for rectangular indentor, 0.9 for semicircular indentor and 0.85 $(\sin\alpha)^{0.5}$ for piers with wedge angles of $2\alpha$ between 60° and 120°, $V_o$ a reference velocity of 1 meter per sound, $\sigma_c$ unconfined compressive strength of ice and A contact area.

Neill(1976) noted that Korzhavin's equation is only for strain rate of $10^{-3}$ to $10^{-4}(sec^{-1})$ defining the effective pressure rage from 0.6 to 1.6 $\sigma_c$. The indentation factor in Korzhaving's equation is idenified as being a function of W/D where W is the overall gross width of the impacting ice sheet.

Afanasev et al.(1971) expressed that the

indentation factor is dependent on the aspect ratio. The calculation of indentation factor, 1, was suggested from the plasticity method by Croasdale el al.(1977). The indentation factor equations for rough and smooth contacts were introduced in this paper. Also Michel and Jolicoeur(1986) have performed tests to determine the indentation coefficient as per the aspect ratio in three failure regions: brittle, transition and ductile.

Table 2.1 Indentation and Contact Coefficients

| Theory | I | k |
|---|---|---|
| Korzhavin (1962) | 2.5 (width > 15D) | 0.4-0.7 |
| Afanasev et al. (1971) | $\sqrt{\frac{5}{\frac{D}{h}}+1}$ | |
| Michel and Toussaint (1977) | 2.97(ductile)<br>2.97(transition)<br>3(brittle) | 0.6-1.0<br>0.25<br>0.3 |
| Croasdale et al. (1977) | 1.45+[ductile)<br>2.97(transition)<br>3(brittle) | 0.6-1.0<br>0.25<br>0.3 |
| Croasdale et al. (1977) | 2.97(C<< h)<br>1.15(D>> h) | |
| Ralston (1978) | 2.97(granular, D<<h)<br>1.15(granular, D>>h)<br>4.12(columnar, D<<h)<br>3.13(columnar, D<<h) | |

However there are disagreements on the individual terms in the above basic Korzhavin's equation. Some coefficients are dependent on the aspect ratio, strain rate, etc. Table 2.1 shows different I and K terms. The indentation factor is now identified as being dependent on the aspect ratio and equal to the plasticity indentation factors. Since the indentation factor from Croasdale et al. (1977) is based on plasticity theory, and additional study for the brittle failure from Afanasev et al. (1971) shows agreement with the values introduced by Allen(1970). However it is larger than other values at low aspect ratio and the failure mode is not classified.

In the case of imperfect contact, the ice force exerts on the local area of the indentor. The calculation of the strain rate of V/D for all cases will not be applicable because D is the total width of indentor and the compressive strength is not the same around the contact conditions. The shape factor also clearly defined because the fracture failure mode can be influenced by the indentor shape.

2) Local Ice Boundary Method

The size and the shape of rubble ice resulting from local and global fracture modes are quite random and dependent on many factors. The following expression shows factors contributing to the geometry of ice blocks when the indentor is imposed by ice load.

$$\delta = f(m, h, v, D, \sigma, \nu_b, d, \alpha)$$

$\delta$ = ice geometry
m = shape factor
$\sigma$ = ice strength(Mpa)
$\nu_b$ = brine volume(o/oo)
d = grain size(mm), and
$\alpha$ = contact angle

The strength of ice includes tensile, shear, flexural, and compressive strengths. The compressive strength of ice depends on strain rate, e, grain size and temperature. The strain rate, e, is an expression of relationship between ice velocity and indentor width. The brine volume

shows the relationship between salinity(o/oo) and temperature(degree). The geometry of rubble is decided by aspect ratio, strain rate, indentor shape and ice properties.

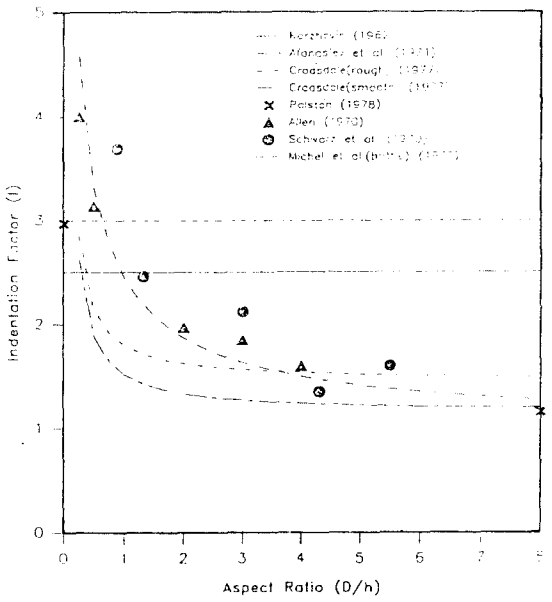


Fig. 2.1 Indentation Factor versus Aspect Ratio

The ice kinetic energy is dissipated by forming fractures which will result in a reduction of load to structures. Unbroken ice contacts a group of rubble ice which fills the space between the indentor and the unbroken sheet ice which is now called a "boundary layer". The size of broken ice can be generated from a random generator assuming that the random sized rubble ice is uniformly distributed around the indentor. This boundary layer thickness can be approximated according to ice failure mode. Based on the measured data from the 1980-1981 Hans Island program, a numerical model was established to investigate the boundary thickness. The boundary thickness ratio(BTR) was studied for the region where the

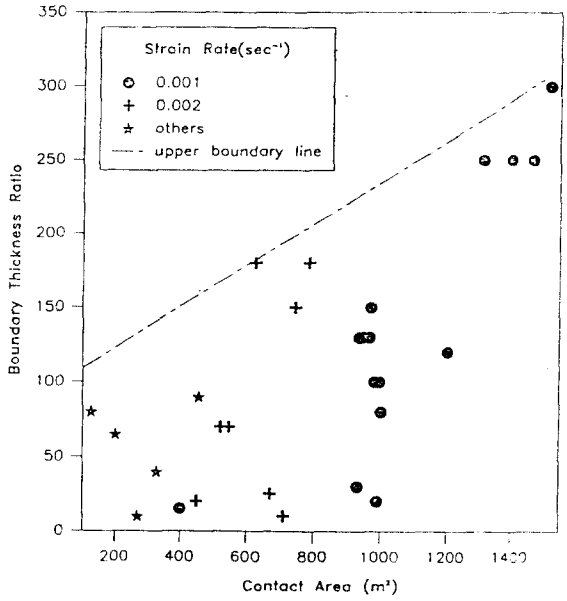


Fig. 2.2 Boundary Thickness Ratio versus Contact Area

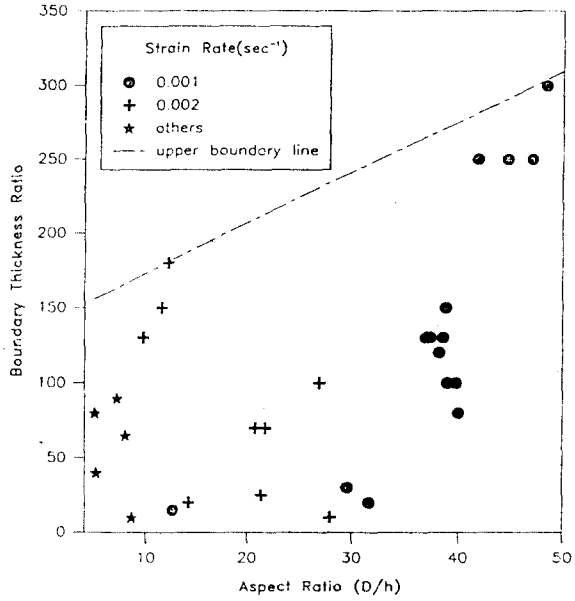


Fig. 2.3 Boundary Thickness Ratio versus Contact Ratio

radial/circumferential cracking and buckling

occur. From this study the maximum BTR was obtained for both cases; contact area and aspect ratio as shown below:

$$BTR = 0.14(A) + 95, \text{ and}$$

$$BTR = 3.42(D/h) + 139$$

Where A is contact area($m^2$).

As shown in Figure 2.2 and 2.3, as the strain rate with constant ratio changes, the ice failure mode changes as well.

Having this boundary layer concept, a method for ice load calculation was developed by Jo(1991). Assuming that random-sized rubble ice is uniformly distributed around the indent for and the maximum rubble size is the same as the thickness of boundary layer, the ice pressure acting on a unit of ice can be expressed as

$$p_i = I_i \sigma_i$$

where $p_i$ is local ice pressure, $I_i$ local indentor coefficient and $\sigma_i$ combination of ice strength. The $\sigma_i$ is an expression of combined ice strength when more than one failure occurs. The flexural strength of ice is important for calculation of ice force for inclined structures and the tensile strength and shear strength for splitting or crackling failure modes.

The total ice force can be written as

$$f_i = p_i D_i k_i m_i$$

where $f_i$ is local ice force, $D_i$ unit local ice projected diameter, $k_i$ local contact coefficent and $m_i$ local ice shape factor. When crushing failure takes place, the indentation factor, I and the contact coefficient, k can be calculated from several ways as shown in Table 2.1. The shape factor m is usually 1 for a flat indentor, 0.9 for semicircular, and $0.85(\sin \alpha)^{0.5}$ for piers with wedge angle of $2\alpha$ between 60° and 120° in crushing mode. in a splitting mode the shape factor is as shown in Table 2.2. When the wedge angle of $2\alpha$ is 60° and 120° in crushing mode. In a splitting mode. So it has a range of 0.25 as the minimum in a splitting mode to 1.0 as the maximum in a crushing mode.

Table 2.2 Shape Factor for Wedge Angle $2\alpha$

| Wedge Angle($2\alpha$) (degree) | Shape Factor (m) |
|---|---|
| 60 | 0.25 |
| 70 | 0.29 |
| 80 | 0.33 |
| 90 | 0.38 |
| 100 | 0.43 |
| 120 | 0.53 |

The total ice pressure acting on the local ice is expressed as

$$P = \sum_{i=1}^{n} I_i \sigma_i = \sum_{i=1}^{n} p_i$$

The total force is also expressed as follows:

$$F = \sum_{i=1}^{n} P_i D_i h K_i m_i = \sum_{i=1}^{n} f_i$$

The n is the number of rubble ice, which arrays about the vicinity of the structure. The local contact coefficent $k_i$ is quite irregular and can be approximated by a random generator which has the maximum and minimum limitations. The friction between unit ice is neglected in the approach but it should be considered as a contributing factor to ice force exerted on the structure in the field. The local ice shape factor $m_i$ is also random. The

maximum value of 1.0 is used for a flat indentor is crushing mode and the minimum of 0.25 with a 60° wedge angle $2\alpha$ in a splitting mode. To calculate the local ice shape factor, a random generator which has an uniform distribution can be used with the maximum and minimum boundaries according to the local ice failure modes. The local indentation factor $I_i$ is dependent on $D_i$ which is the local unit ice projected diameter and can be obtained by using a formula.

3) Proportional Failure Method

Ice fails with any combination of failure modes. The theories for ice forces and pressures are normally based on a single mode which rarely occurs in nature. Based on the ice failure map, the ice failure mode can be approximated.

For the pure crushing zone, the proportional factor for crushing mode is expressed as $\pi_c$ with the maximum of 1. As the failure mode enters the cracking zone, $\pi_c$ decreases and $(1-\pi_c)$ will increase. As the failure mode grades into the pure cracking/no-crushing zone, the $(1-\pi_c)$ value goes up and the tensile strength ($\sigma_t$) becomes dominant. The tensile strength of ice is much smaller than the compressive strength. The formula for ice strength can be expressed as

$$\sum i = \sigma_c \pi_c + \sigma_t (1-\pi_c)$$

The ice pressure is

$$P = I\sum i = I[\ \sigma_c \pi_c + \sigma_t (1-\pi_c)]$$

The ice force from a proportional failure method based on two failures, crushing and cracking can be expressed as

$$F = PDhkm = I[\ \sigma_c \pi_c + \sigma_t (1-\pi_c)]\ Dhkm$$

## 3. ICE FORCE COMPARISON

During 1980 to 1981, the actual ice loads were measured in Hans Island. Also other information like ice velocity, thickness, contact width and contact area were obtained as well. In this paper, the three methods(Korzhavin, Local Boundary, and Proportional Failure Methods) were used in the estimation of ice loads and the results were compared. Table 3.1 shows a example of the results. In Table 3.1, $F_m$ is measured ice force (MN), $F_c$ crushing ice force (MN), $F_p$ ice force predicted from the Proportional Failure Method(MN), $F_l$ ice force estimited from the Local Boundary Method(MN), D/h aspect ratio, e strain rate($sec^{-1}$), D contact width (m), V ice velocity (m/s), h ice thickness(m), CA contact area(DA) ($m^2$) and m shape factor 0.9. Since the output is of quite large volume, only one table is introduced in this paper.

Table 3.1 Ice Force Comparison

| B.T.R. | $F_l$(k=0.2)(MN) | $F_l$(k=0.3)(MN) |
|---|---|---|
| 5 | 3.1 | 4.7 |
| 10 | 19.8 | 29.7 |
| 20 | 29.2 | 43.8 |
| 30 | 35.6 | 53.4 |
| 40 | 39.6 | 59.4 |
| 50 | 59.6 | 89.4 |

Where:
$F_m$=24(MN), $F_c$=319(MN), $F_p$=164(MN),
D/h=14.3, e=0.002($sec^{-1}$), $D^p$=80(m)
V=0.39(m/s), h=5.6(m), CA=450($m^2$)

The results show that the Korzhavin method highly over-estimates ice loads, the Proportional

Failure Method also over-estimates but not as much as Korzhavin's method and the Local Boundary Method estimates very close to the actually measured data.

## 4. EXPERIMENTAL MODELLING

A physical model study of an icebreaking tanker moored to an offshore SPM terminal in moving ice was conducted in the "Wartsila" Arctic Research Centre in Helsinki, Finland. The model study was conducted to determine the behaviour of the icebreaking tanker moored to a SPM terminal in moving ice.

A series of model tests were conducted in the WARC test facility. The ice tank basin was 29 m long, 4.8 m wide and 1.4 m deep. A 1:40 model was used in the tests. The main dimensions of the model are presented below:

$$\begin{aligned} Lcwl &= 3.751\,m \\ Bcwl &= 0.538\,m \\ Tcwl &= 0.238\,m \\ \triangle &= 0.354\,m^3 \end{aligned}$$

The experimental set up is as shown in Figure 4.1.

An ice sheet for tests was grown in the ice test facility. The target thickness of the level ice sheet ws 18 to 23 mm with a flexural strength of around 10 kpa. Once the ice properties were established two holes were sawn into the inbroken ice sheet. The SPM terminal and icebreaking tanker model were then positioned into the pre-sawn holes and all mechanical and electrical connections were made. The ice sheet was then pushed against the SPM terminal and icebreaking tanker model using a second auxiliary carriage. The target pushing speed of the level ice was 27 mm/sec.

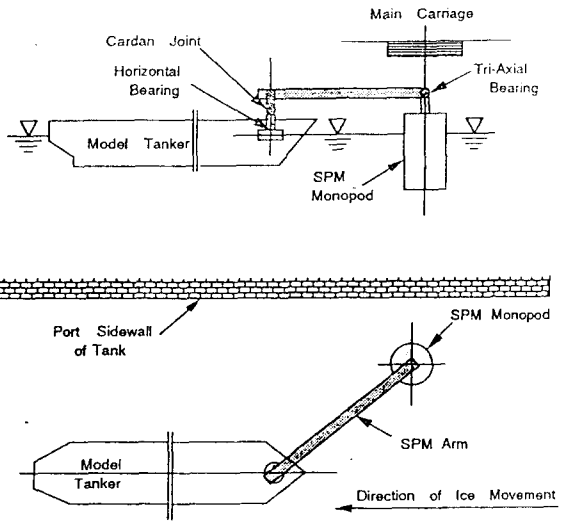


Fig. 4.1 Physical Modeling Set Up

Based on the three methods (Crushing, Local ice Boundary and Proportional Failure methods), the ice forces on the icebreaking tanker moored to a SPM terminal were obtained. The results were applied to investigate the ice and tanker interaction problem.

In the crushing method, the shape factor I, which is the same as for a rectangular body, was used. In the proportional approach, the $\pi_c$ term of 1 was applied. This was due to the fact that the strain rate falls mostly in the cracking region for the ice failure map. In the local ice boundary method, a B.T.R. of 20 was utilized. The added mass of the tanker was approximated from the two dimensional added mass equation i calm water. To apply two dimensional results to the three dimensional case, the strip theory was adapted. The drag coefficient of a submerged cubic was applied to approximate the damping coefficient. The taker was divided into 17 sections to calculate the damping force of each section since the angular velocity due to the ice load changes for each section. Calculation of ice forces depend on the projected of the tanker. The projected area was calculated

from calculated from the angle between the ice direction and the tanker.

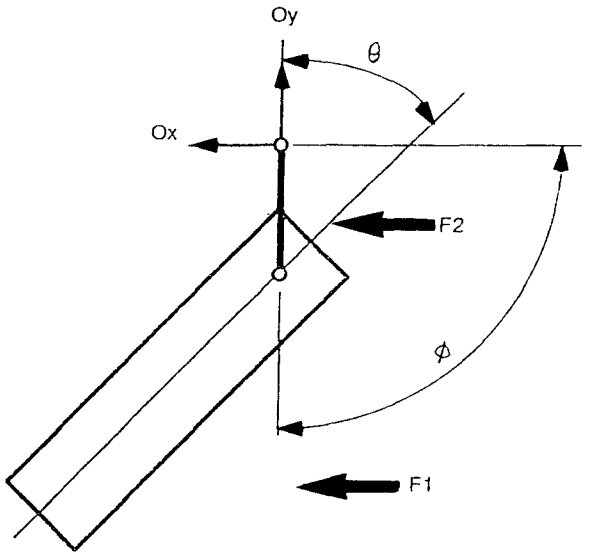


Fig. 4.2 Notation of Numerical Model

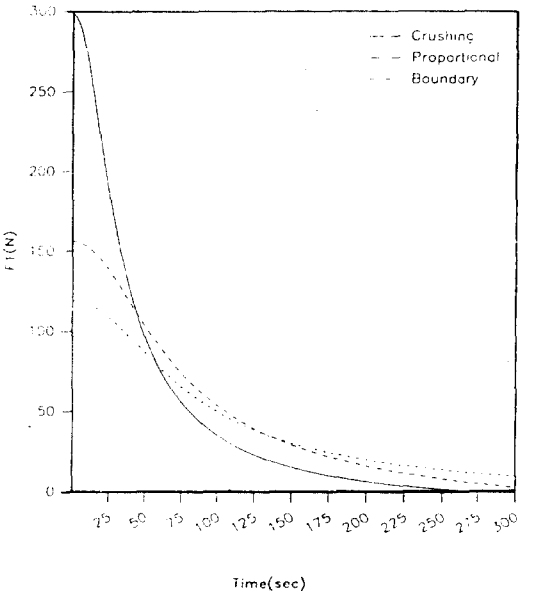


Fig. 4.4 Time versus F1, Model # 1

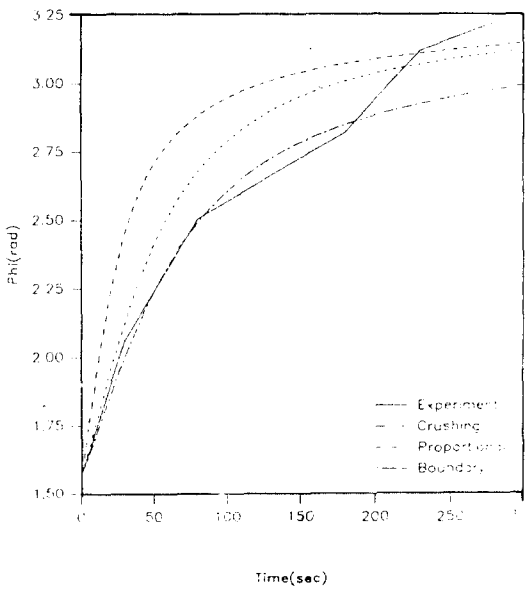


Fig. 4.3 Time versus $\phi$ Model # 1

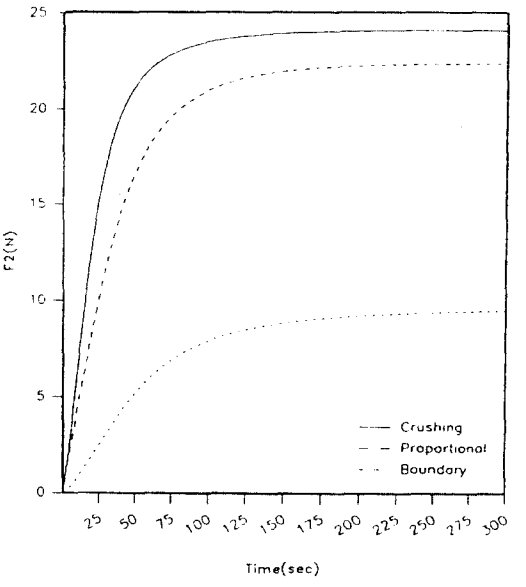


Fig. 4.5 Time versus F2, Model # 1

Figure 4.2 shows the notation of numerical model. In model 1, $\phi$ was 45°, $\theta$ 45° level ice

thickness 18.5 mm and ice velocity 27 mm/sec. In model 2, $\phi$ was 90°, $\theta$ 0°, level ice thickness 22.5 mm and ice velocity 27 mm/sec. In Figure 4.3 to 4.12 results from the three different methods were compared with the data from the physical experiment. Figures 4.3 and 4.8 show the comparison of the angle between the ice direction and the tanker moored to an SPM terminal.

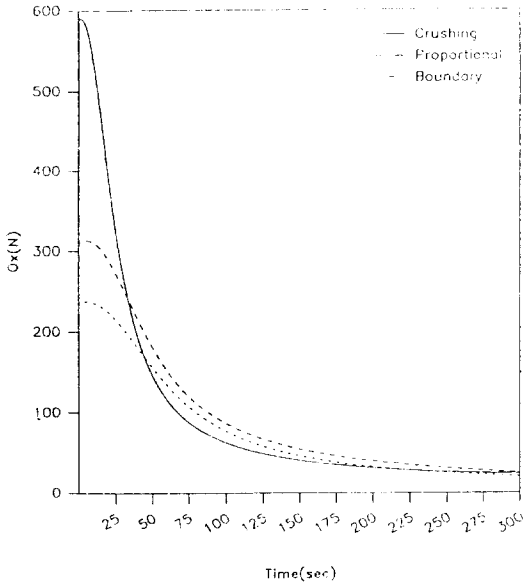


Fig. 4.6 Time versus OX, Model # 1

Figure 4.5 and 4.8 show that the ice forces from the crushing failure method are over-estimated, thus the movement of the tanker is over-predicted.

Figure 4.4, 4.5, 4.9 and 4.10 show the results of calculated ice forces on a tanker using the three different methods. Ice forces acting on the monopode arm connected to the terminal are shown in Figures 4.6, 4.7, 4.11 and 4.12. It is evident from Figures 4.3 to 4.12 that the crushing failure method over-estimates ice loads thus the move-ments of the tanker are over-predicted. The movement of the tanker were relatively well predicted form the proportional failure and the local ice boundary methods.

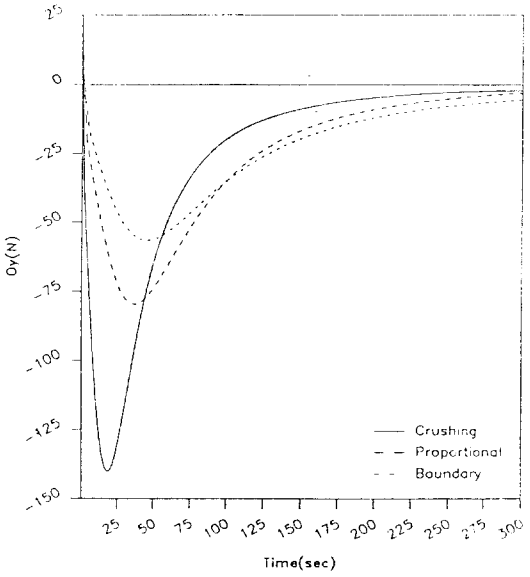


Fig. 4.7 Time versus OY, Model # 1

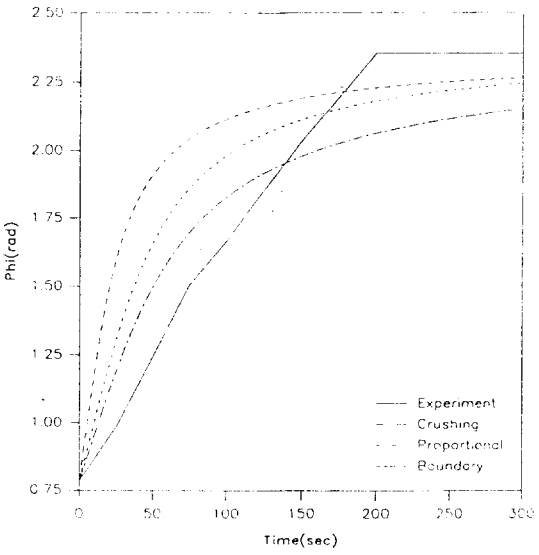


Fig. 4.8 Time versus $\phi$, Model # 2

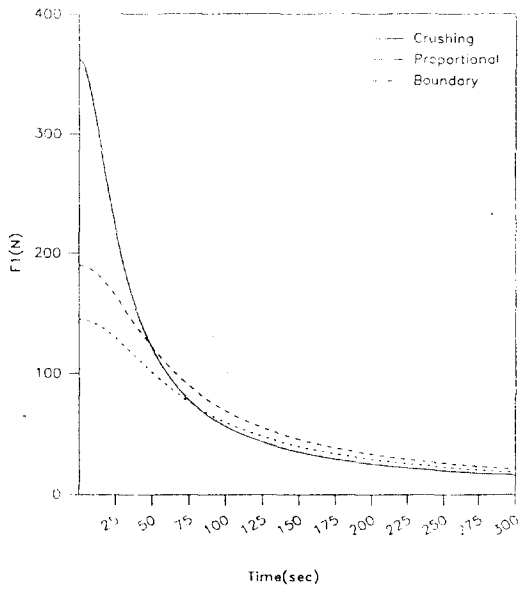


Fig. 4.9 Time versus F1, Model # 2

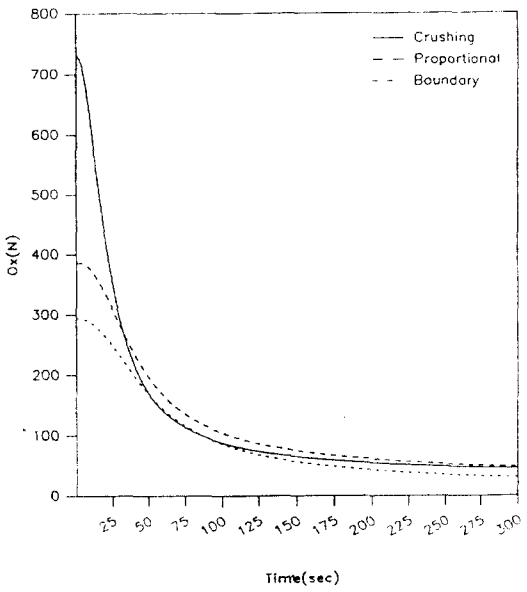


Fig. 4.11 Time versus OX, Model # 2

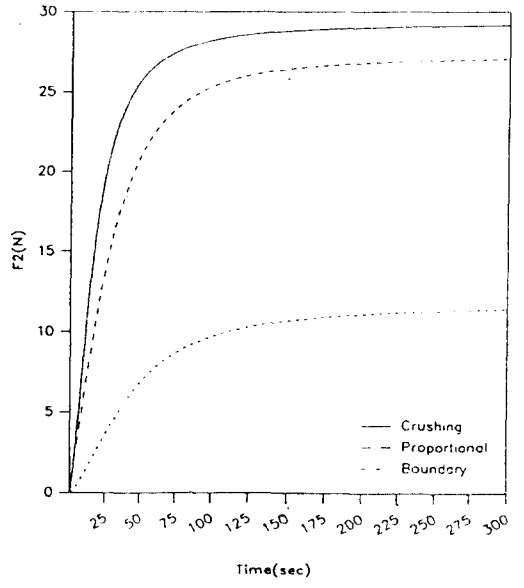


Fig. 4.10 Time versus F2, Model # 2

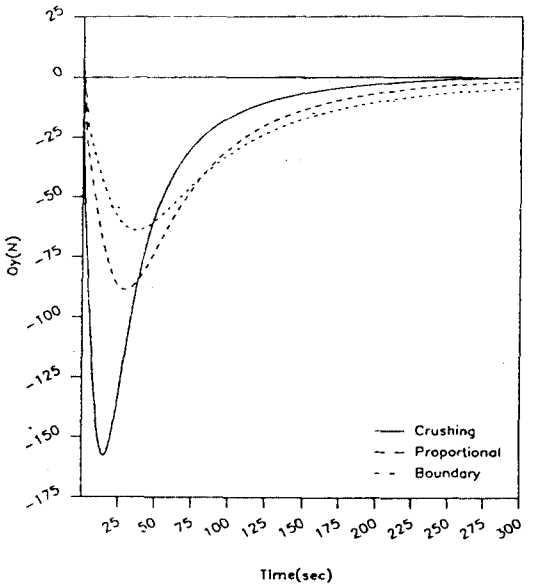


Fig. 4.12 Time versus OY, Model # 2

## 5. CONCLUSION

The well known method from Korzhavin's concept over-predicts the ice loads. The Local Boundary and Proportional Failure Methods can be applied in the estimation of ice loads not only to fixed structures but also to moving structures. The ice loads from the Local Boundary compare very closely to the actual measurements both from Hans Island and from the experiments. Over-prediction of ice loads led a fast movement or vanning of the tanker moored to SPM system. The accurate or close estimation of ice loads is critical to the design of ice structures and prediction of behaviour of moving structures in the ice region.

## REFERENCES

1) Afanasev, V.P., Dogopolov, Y.V., and Shraishtein, Z.I. 1971. "Ice Pressure on Individual Marine Structures." Ice Physics and Ice Engineering, Israel Program for Scientific Translation, 1973, pp. 50-68.
2) Allen, J.L. 1970. "Effective Force of Floating Ice on structures." National Research Council of Canada, Technical Memorandum 98, Ottawa.
3) Croasdale, K.R., Morgenstern, N.R., and Nuttall, J.B. 1977. "Indentation Tests to Investigate Ice Pressures on Vertical Piers." Journal of Glaciology 19(81), pp. 301-312.
4) Jo, C.H. 1991. "Study of Shape Factor for Reducing Ice Force on Arctic Structure and Ice Force Prediction for Combined Ice Failure", Proc. of OTC Conference, Vol.VI, Houston, pp. 185- 192.
5) Korzhavin, K.N. 1962. "Action of Ice on Engineering Structure" USSR Acad. Sci. Siberian Branch. CRREL Draft Translation No. 260, Hanover, NH, 1971.
6) Michel, B. and Jolicoeur, L. 1986. "Experimental Study of Indentation of Columnar Grained Ice Sheets in the Transition Zone." Proc. of OMAE Symp., Vol. IV, Tokyo, pp. 479-485.
7) Michel, B. and Toussaint, N. 1977. "Mechanisms and Theory of Indentation of Ice Plates." Journal of Glaciology, Vol. 19, No.81, pp. 285-301.
8) Neil, C.R. 1976. "Dynamic Ice Forces on Piers and Piles. An Assessment of Design Guidelines in the Light Recent Research." Canadian Journal of Civil Engineering, Vol.3, No.2, pp. 305-341.
9) Ralston, T.D. 1979. "An Analysis of Ice Sheet Indentation." Proc. IAHR Ice Symp., Vol.I, Lulea, Sweden, pp. 13-31.
10) Schwarz, J. 1970. "The Pressure of Floating Ice Fields on Piles." Proc. of the International Association of Hydraulic Research Ice Symposium, No.6-3, Reykjavik, Iceland, p. 12.